

THEORETICAL ANALYSIS OF A DIPOLE-FED HORN ANTENNA

G.V. Eleftheriades, Walid Ali-Ahmad, L.P.B. Katehi, G.M Rebeiz

Center for Space Terahertz Technology,
University of Michigan, Ann Arbor, MI

March 1990

Abstract

This antenna consists of a strip dipole printed on a membrane and suspended in an etched pyramidal silicon cavity. The entire fabrication is monolithic. For the theoretical characterization, the horn is approximated by a stepped structure of multiple rectangular waveguide sections. The fields in each section are given by a linear combination of waveguide modes, and the fields in air are given by a continuous plane wave spectrum. To evaluate the Green's function for this problem, an infinitesimally small electric dipole is considered in one of the waveguide sections. Then, the fields inside the silicon cavity are evaluated, and the far-field patterns are found from the Fourier transforms of the electric field on the aperture of the horn.

1. INTRODUCTION

In millimeter wave imaging systems the use of a single detector with electronic or mechanical scanning is inadequate. The events may be too fast, or the required integration time too long. The way to eliminate this limitation is to image all points simultaneously. In 1987, G.M. Rebeiz fabricated a monolithic millimeter-wave imaging array consisting of a large number of silicon horns with detectors placed at the focal plane of the imaging system. For the design of this array, the radiating elements were characterized experimentally and mutual coupling was neglected. As a result, the efficiency of the array was approximately 45 percent. To improve the performance of the array, the elements have to be modeled accurately. This paper presents the development of a rigorous method for the theoretical characterization of the isolated elements.

The procedure for rigorously generating the Green's function for a dipole-fed metallic rectangular horn radiating in free-space is being described. The method allows for step discontinuities to be included in the horn geometry and is not limited by large flaring angles or short axial lengths.

2. THEORY

The procedure which has been employed in the formulation of the problem consists of five steps:

1. The geometry of the horn is approximated by a cascade of rectangular waveguide steps. One of the waveguide steps contains an infinitesimal dipole excitation.
2. The field on the apex and aperture of the horn is transferred, via appropriate transmission matrices, on the excitation (source) plane.
3. The aperture field is matched to free space using plane-wave expansion.
4. The transferred fields of step two are matched over the excitation plane.
5. Finally steps (3) and (4) combined together result in a linear system of equations. The solution of this system provides the required Green's function in discrete form inside the horn and in continuous form in the half space.

2.1 Approximation of the horn geometry

The horn is approximated by a multisteped discontinuity consisting of N sections as shown in Figure 1.

The horn aperture lies on an infinite-metallic screen. Furthermore, it is assumed that there is no reflection from the apex of the horn, since any reflection will be at cut-off.

2.2 Transfer of the apex and Aperture Field on the source plane

Each step discontinuity is characterized by a transmission matrix $[T_b]$:

$$\begin{bmatrix} B^{(2)} \\ D^{(2)} \\ A^{(2)} \\ C^{(2)} \end{bmatrix} = [T_b] \begin{bmatrix} B^{(1)} \\ D^{(1)} \\ A^{(1)} \\ C^{(1)} \end{bmatrix} \quad (1)$$

where the elements of the column matrices denote the unknown coefficients of the field next to the discontinuity. The field in each waveguide is represented in a modal expansion as shown below :

$$\begin{aligned} \bar{E}_t^{(i)} &= \sum_{m,n} \left[\bar{e}_{mn}^{(i),TE}(x,y) \left\{ A_{mn}^{(i)} e^{-\gamma_{mn}^{(i)} z} + B_{mn}^{(i)} e^{\gamma_{mn}^{(i)} z} \right\} \right. \\ &\quad \left. + \bar{e}_{mn}^{(i),TM}(x,y) \left\{ C_{mn}^{(i)} e^{-\gamma_{mn}^{(i)} z} + D_{mn}^{(i)} e^{\gamma_{mn}^{(i)} z} \right\} \right] \end{aligned} \quad (2)$$

$$\begin{aligned} -\hat{z} \times \bar{H}_t^{(i)} &= \sum_{m,n} \left[\bar{e}_{mn}^{(i),TE}(x,y) Y_{mn}^{(i),TE} \left\{ A_{mn}^{(i)} e^{-\gamma_{mn}^{(i)} z} - B_{mn}^{(i)} e^{\gamma_{mn}^{(i)} z} \right\} \right. \\ &\quad \left. + \bar{e}_{mn}^{(i),TM}(x,y) Y_{mn}^{(i),TM} \left\{ C_{mn}^{(i)} e^{-\gamma_{mn}^{(i)} z} - D_{mn}^{(i)} e^{\gamma_{mn}^{(i)} z} \right\} \right] \end{aligned} \quad (3)$$

where i takes the values 1 or 2.

In the above representation both TE and TM modes are included to support the analysis of an arbitrary planar excitation current. A cascade of such transmission matrices, along with associated phase delay transmission matrices is used to transfer the apex and aperture field on the excitation plane :

$$\begin{bmatrix} B^I \\ D^I \\ A^I \\ C^I \end{bmatrix} = [T_B] \begin{bmatrix} B^{(1)} \\ D^{(1)} \\ 0 \\ 0 \end{bmatrix}_{\text{apex}} \quad \begin{bmatrix} B^{II} \\ D^{II} \\ A^{II} \\ C^{II} \end{bmatrix} = [T_A] \begin{bmatrix} B^{(N)} \\ D^{(N)} \\ A^{(N)} \\ C^{(N)} \end{bmatrix}_{\text{aperture}} \quad (4)$$

Referring to fig.1, the source interface divides the source section #K into two subsections. one on the left, having length l_I and one on the right, having length l_{II} . Accordingly, in equations (4) above, the modal coefficients of the left subsection are denoted with the index (I) and those of the right subsection with the index (II).

2.3 Matching to Half space

This task matches the discrete field spectrum of the aperture section of the horn to the continuous field spectrum of free space, over the horn aperture. The field in free-space is expressed as a plane wave superposition:

$$\bar{E}(x, y, z) = \frac{1}{2\pi} \int_{-\infty}^{\infty} \int_{-\infty}^{\infty} \bar{g}(k_x, k_y) e^{-ik_x x} e^{-ik_y y} e^{-ik_z z} dk_x dk_y \quad (5)$$

with the transverse component of $\bar{g}(k_x, k_y)$ given by:

$$\bar{g}_t(k_x, k_y) = \frac{1}{2\pi} \int \int_{\text{aperture}} \bar{E}_t(x, y, 0^+) e^{ik_x x} e^{ik_y y} dx dy \quad (6)$$

Field continuity on the aperture of the horn leads to the following matrix equation :

$$\begin{bmatrix} F_{11} & F_{12} & F_{13} & F_{14} \\ F_{21} & F_{22} & F_{23} & F_{24} \end{bmatrix} \begin{bmatrix} B^{(N)} \\ D^{(N)} \\ A^{(N)} \\ C^{(N)} \end{bmatrix} = \begin{bmatrix} 0 \\ 0 \\ 0 \\ 0 \end{bmatrix} \quad (7)$$

The submatrices F_{ij} contain reaction integrals involving the discrete modes of the aperture field. There are three kind of reaction integrals as shown below :

$$I_{ijmn}^{pq} = \int_{-\infty}^{\infty} \int_{-\infty}^{\infty} \frac{(k^2 - k_y^2)}{k_z} \bar{e}_{xij}^p(k_x, k_y) \bar{e}_{xmn}^{*q}(k_x, k_y) dk_x dk_y \quad (8)$$

$$I_{2ijmn}^{pq} = \int_{-\infty}^{\infty} \int_{-\infty}^{\infty} \frac{(k^2 - k_x^2)}{k_z} \tilde{e}_{yij}^p(k_x, k_y) \tilde{e}_{ymn}^{*q}(k_x, k_y) dk_x dk_y \quad (9)$$

$$I_{3ijmn}^{pq} = \int_{-\infty}^{\infty} \int_{-\infty}^{\infty} \frac{k_x k_y}{k_z} [\tilde{e}_{yij}^p(k_x, k_y) \tilde{e}_{xmn}^{*q}(k_x, k_y) + \tilde{e}_{xij}^p(k_x, k_y) \tilde{e}_{ymn}^{*q}(k_x, k_y)] dk_x dk_y \quad (10)$$

where p, q take the values 1 ($\rightarrow TE$) or 2 ($\rightarrow TM$).

In order to facilitate the numerical evaluation of the integrals it is advantageous to transform them in the space-domain. Their transformation from the spectral-domain to the spatial-domain is accomplished via the application of Parseval's theorem leading to :

$$I_{1ijmn}^{pq} = \frac{1}{2\pi} \int_{x_N}^{x_N} \int_{-y_N}^{y_N} \frac{ie^{-ik\rho}}{\rho} (k^2 + \frac{\partial^2}{\partial y^2}) [e_{x1ij}^p(-x) \otimes e_{x1mn}^q(x)] [e_{x2ij}^p(-y) \otimes e_{x2mn}^q(y)] dx dy \quad (11)$$

$$I_{2ijmn}^{pq} = \frac{1}{2\pi} \int_{x_N}^{x_N} \int_{-y_N}^{y_N} \frac{ie^{-ik\rho}}{\rho} (k^2 + \frac{\partial^2}{\partial x^2}) [e_{y1ij}^p(-x) \otimes e_{y1mn}^q(x)] [e_{y2ij}^p(-y) \otimes e_{y2mn}^q(y)] dx dy \quad (12)$$

$$I_{3ijmn}^{pq} = -\frac{1}{2\pi} \int_{x_N}^{x_N} \int_{-y_N}^{y_N} \frac{ie^{-ik\rho}}{\rho} \frac{\partial^2}{\partial x \partial y} [(e_{y1ij}^p(-x) \otimes e_{x1mn}^q(x)) (e_{y2ij}^p(-y) \otimes e_{x2ij}^q(y)) + (e_{x1ij}^p(-x) \otimes e_{y1mn}^q(x)) (e_{x2ij}^p(-y) \otimes e_{y2mn}^q(y))] dx dy \quad (13)$$

where $\rho = \sqrt{x^2 + y^2}$.

2.4 Matching on the source interface

The point excitation is assumed to be a y-directed surface current given by:

$$\vec{K}(x, y) = \delta(x - x') \delta(y - y') \hat{y} \quad (14)$$

Upon matching over the source interface we derive the matrix equation :

$$[A] \begin{bmatrix} B^{(I)} \\ D^{(I)} \\ A^{(I)} \\ C^{(I)} \end{bmatrix} = [A] \begin{bmatrix} B^{(II)} \\ D^{(II)} \\ A^{(II)} \\ C^{(II)} \end{bmatrix} + \begin{bmatrix} 0 \\ 0 \\ e_{1mn}^{TE}(x', y') \\ e_{2mn}^{TM}(x', y') \end{bmatrix} \quad (15)$$

where matrix [A] above involves the mode admittances of the source section as shown below :

$$\begin{bmatrix} I & O & I & O \\ O & I & O & I \\ -Y^{TE,K} & O & Y^{TE,K} & O \\ O & -Y^{TM,K} & O & Y^{TM,K} \end{bmatrix} \quad (16)$$

2.5 Derivation of the final system of equations

The equations that have been generated so far are summarized below :

- Apex-aperture field transferred on the source plane through transmission matrices:

$$\begin{bmatrix} B^{(I)} \\ D^{(I)} \\ A^{(I)} \\ C^{(I)} \end{bmatrix} = [T_B] \begin{bmatrix} B^{(1)} \\ D^{(1)} \\ 0 \\ 0 \end{bmatrix}_{\text{apex}} \quad \begin{bmatrix} B^{(II)} \\ D^{(II)} \\ A^{(II)} \\ C^{(II)} \end{bmatrix} = [T_A] \begin{bmatrix} B^{(N)} \\ D^{(N)} \\ A^{(N)} \\ C^{(N)} \end{bmatrix}_{\text{aperture}} \quad (17)$$

- Matching of the aperture field :

$$[F] \begin{bmatrix} B^{(N)} \\ D^{(N)} \\ A^{(N)} \\ C^{(N)} \end{bmatrix} = \begin{bmatrix} 0 \\ 0 \\ 0 \\ 0 \end{bmatrix} \quad (18)$$

- Matching of the fields on the source interface :

$$[A] \begin{bmatrix} B^{(I)} \\ D^{(I)} \\ A^{(I)} \\ C^{(I)} \end{bmatrix} = [A] \begin{bmatrix} B^{(II)} \\ D^{(II)} \\ A^{(II)} \\ C^{(II)} \end{bmatrix} + \begin{bmatrix} 0 \\ 0 \\ e_{1mn}^{TE}(x', y') \\ e_{2mn}^{TM}(x', y') \end{bmatrix} \quad (19)$$

The above equations are merged together to form a single matrix equation involving the modal coefficients of the apex and aperture sections :

$$\begin{bmatrix} [A][T_B]' & -[A][T_A] \\ O & [F] \end{bmatrix} \begin{bmatrix} B^{(1)} \\ D^{(1)} \\ B^{(N)} \\ D^{(N)} \\ A^{(N)} \\ C^{(N)} \end{bmatrix} = \begin{bmatrix} O \\ O \\ e_1 \\ e_2 \\ O \\ O \end{bmatrix} \quad (20)$$

Note that the block-submatrix $([A][T_B])'$ consists only of the half first columns of $[A][T_B]$. This is a consequence of the assumption of no reflections from the apex of the horn. Having found the modal coefficients of the apex and aperture sections, the Green's function inside the horn is represented as a discrete Fourier series whereas outside the horn as a Fourier integral. Specifically the transverse component of the Green's function for a y-directed current inside the horn can be represented in a quadratic form as shown below :

$$\bar{G}_t(x, y, x', y') = \begin{bmatrix} \bar{e}_{mn}^{TE}(x, y) & \bar{e}_{mn}^{TM}(x, y) & \bar{e}_{mn}^{TE}(x, y) & \bar{e}_{mn}^{TM}(x, y) \end{bmatrix} [T_B][SM1] \begin{bmatrix} 0 \\ 0 \\ e_{mn}^{TE}(x', y') \\ e_{mn}^{TM}(x', y') \end{bmatrix} \quad (21)$$

In the above representation [SM1] is an appropriate submatrix of the inverse of the system matrix defined in (19).

3. NUMERICAL RESULTS

The aperture field and the far-field for a specific horn geometry has been evaluated. For this purpose the aperture coefficients are calculated from the solution of matrix equation (20). For a vertical point source only modes of the form (m,n) [m=1,3,5, ... and n=0,2,4, ...] are excited. Numerical convergence for the far-field was achieved when TE and TM modes up to the order (7,7) were included. The magnitude of the co-polarized aperture field

shown in fig.4 is recognized to be a perturbed dominant mode field distribution. Furthermore, the utilization of both TE and TM modes in the theory enabled the calculation of the cross-polarized aperture field which has a level of -16dB for the case under consideration. The phase of the aperture field is depicted in fig.5. Of interest is the cross-polarization phase which divides the aperture, along its geometrical axes of symmetry, into four quadrants. Each quadrant is out of phase with its adjacent quadrants.

4. CONCLUSION

This paper presented a rigorous method for the characterization of a monolithic horn antenna excited by an infinitesimal small dipole printed on a membrane. Using this method, the fields on the aperture of the silicon horn were evaluated and transformed to the Fourier domain in order to derive the far-field patterns. The developed method may easily be extended to compute input impedance and resonant properties of these radiating structures for feeding dipoles of finite size.

5. ACKNOWLEDGMENTS

The work was sponsored by the Center for Space Terahertz Technology, the University of Michigan, Ann Arbor, MI.

REFERENCES

1. Thomas Wriedt, Karl-Heinz Wolff, Frint Arndt and Ulrich Tucholke, "Rigorous Hybrid Field Theoretic Design of Stepped Rectangular Waveguide Mode Converters Including the Horn Transitions into Half-Space," *IEEE Transactions on Antennas and Propagation*, Vol. 37, No. 6, June 1989.
2. Amir I. Zaghoul and Robert H. MacPhie, "Cross-Correlation Formulation of the Complex Power from Planar Apertures," *Radio Science*, Vol. 10, No. 6, pp. 619-624, June 1975.
3. Robert H. McPhie and Amir I. Zaghoul, "Radiation from a Rectangular Waveguide with Infinite Flange-Exact Solution by the Correlation Matrix Method," *IEEE Transactions of Antennas and Propagation*, Vol. AP-28, No. 4, July 1980.
4. Jose A. Encinar and Jesús Rebolgar, "A Hybrid Technique for Analyzing Corrugated and Non-Corrugated Rectangular Horns," *IEEE Transactions on Antennas and Propagation*, Vol. AP-34, No. 8, August 1986.

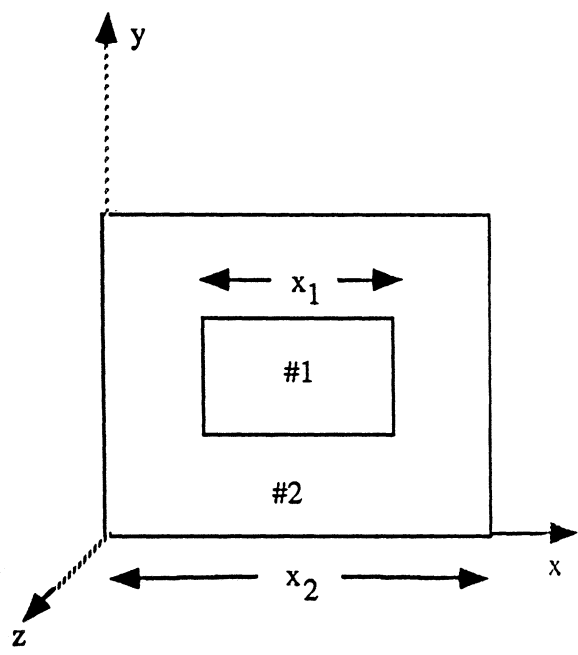
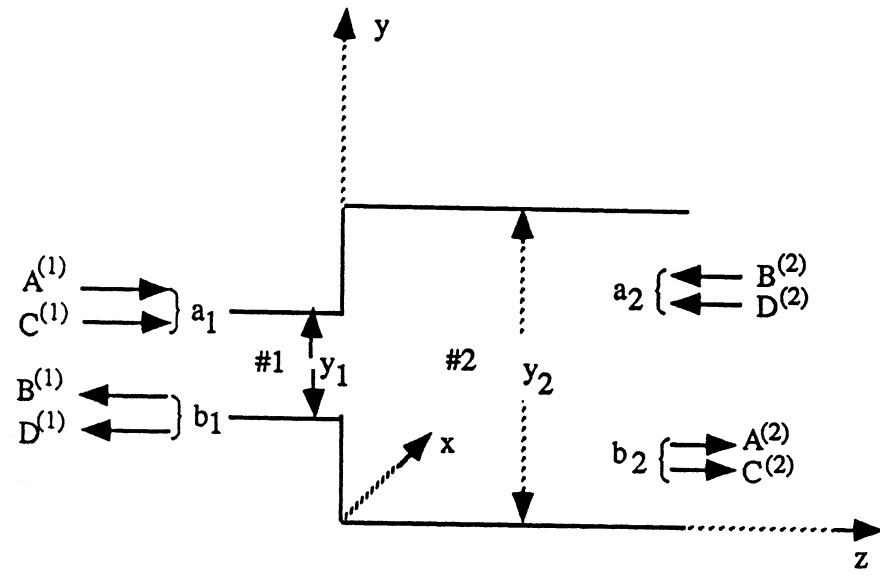


Fig.1 A waveguide step discontinuity.

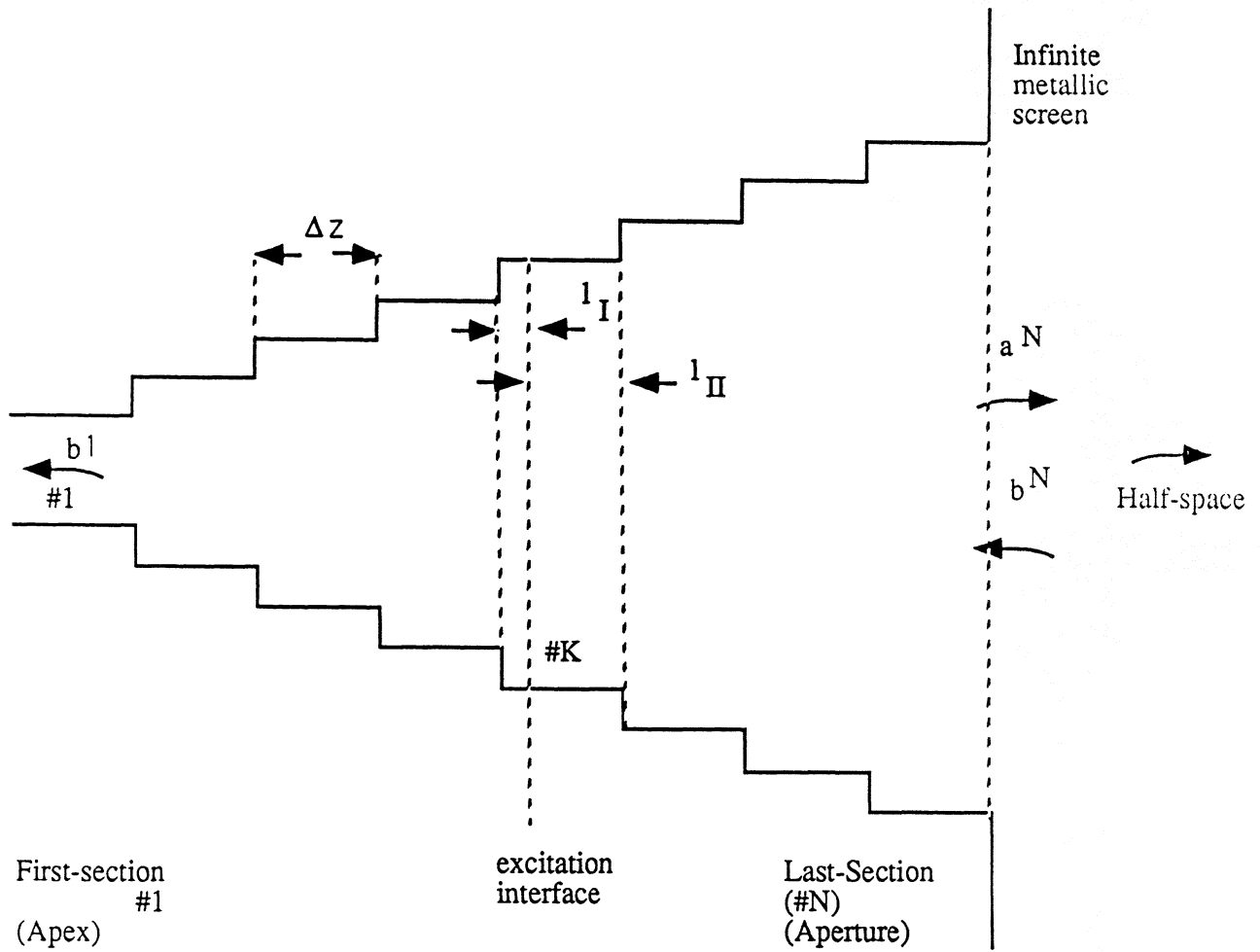


Fig.2 Approximation of the horn geometry by cascaded step discontinuities.

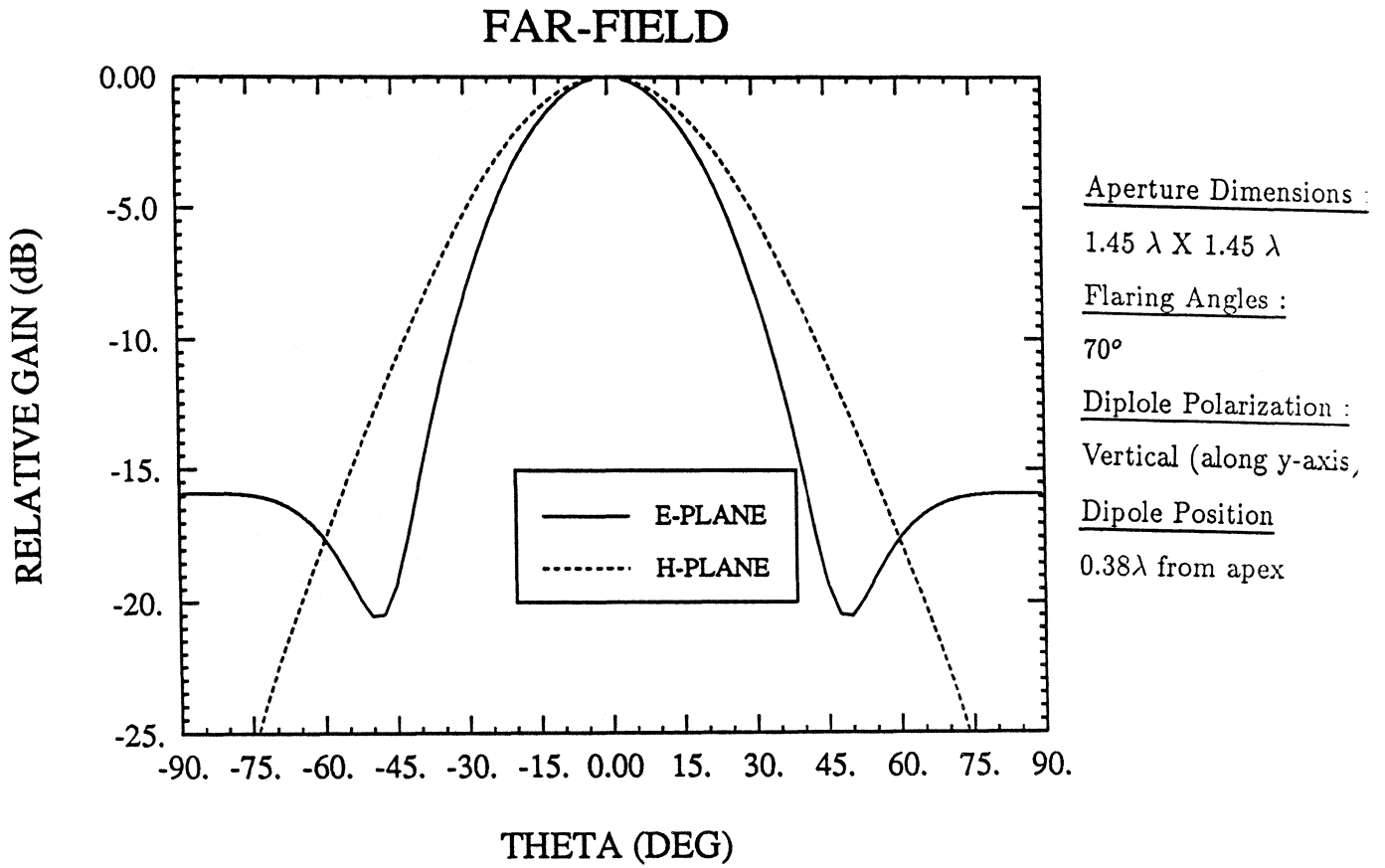
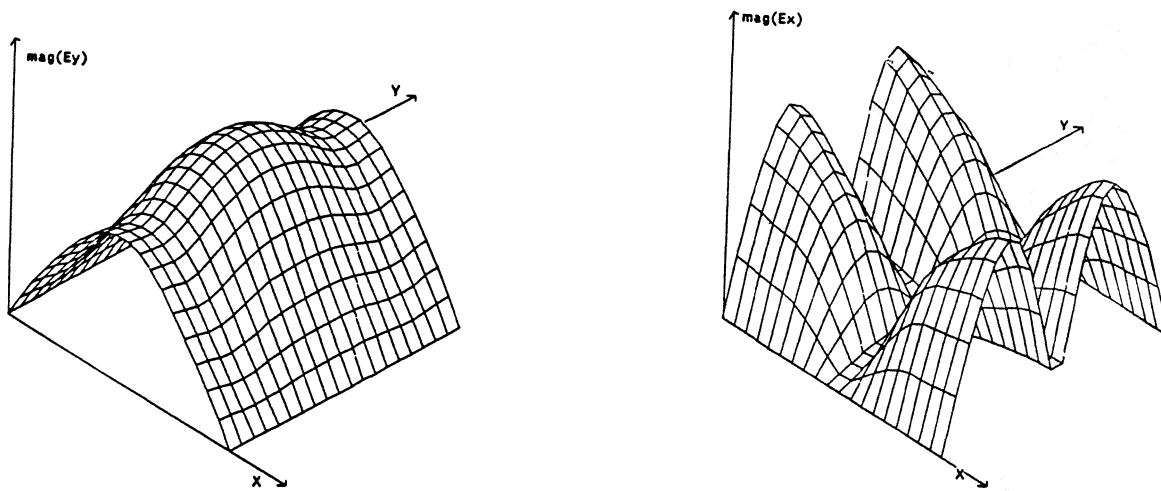


Fig.3 Far-field.



MAGNITUDE OF E-FIELD ALONG APERTURE DIAGONAL

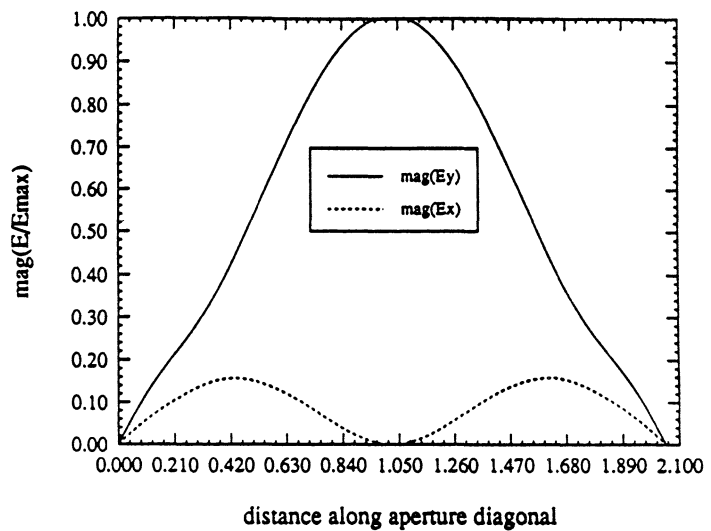


Fig.4 Magnitude of aperture field. (a) The co-polarized field. (b) The cross-polarized field. (c) Comparison of the co-polar and cross-polar magnitude along the aperture diagonal.

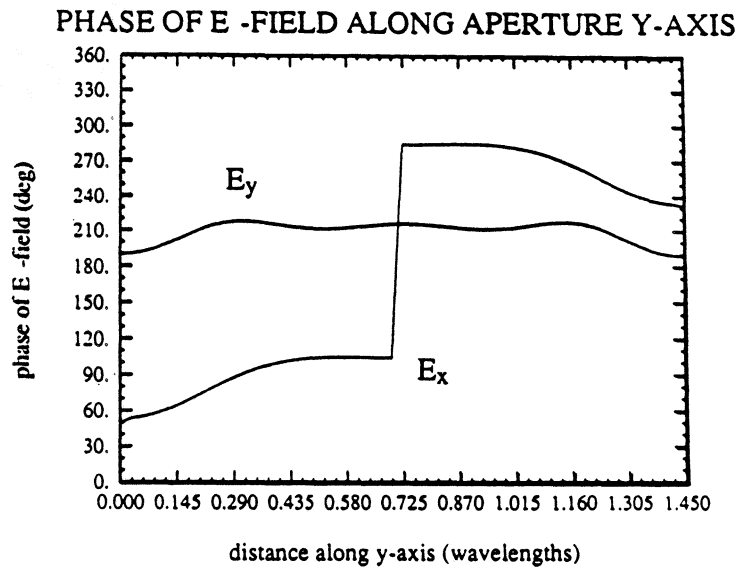
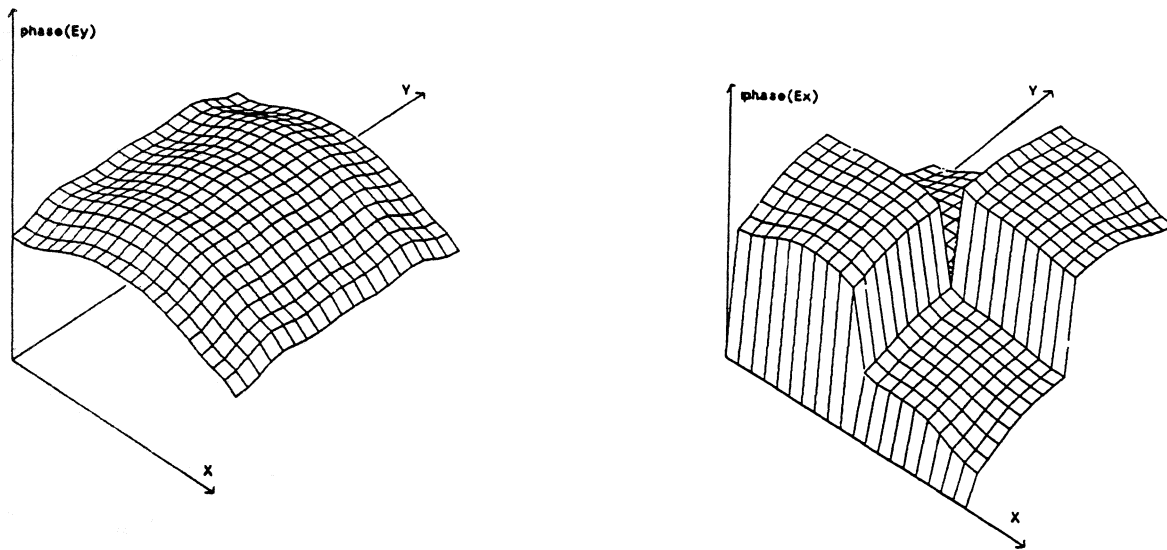


Fig.5 Phase of aperture field. (a) The co-polarized field. (b) The cross-polarized field. (c) Comparison of the co-polar and cross-polar phase along the aperture diagonal.